A Generalized Discrete-Vortex Method for Sharp-Edged Cylinders

P. K. Stansby*
University of Manchester, Manchester, England, U.K.

An improved scheme for introducing vortex sheets from the sharp edges of a cylinder represented in an inviscid calculation by the panel method is described. Three edge conditions are satisfied directly through an efficient iterative formulation, while a fourth is satisfied approximately. The cylinder surface is represented only by a vortex sheet and nascent vorticity is also treated as elements of vortex sheet. Vorticity in the wake is handled by the vortex-in-cell method with overlapping meshes for good definition. The method is tested with various shapes which incorporate two shedding edges (an equilateral triangle and a range of rectangles).

Introduction

SEVERAL methods have been used to simulate time-dependent separated flows around cylindrical bodies. Time-stepping solutions of the Navier-Stokes equations in the form of a vorticity equation have been made through Eulerian schemes,[1] Lagrangian schemes,[2,3] and a hybrid scheme, Eulerian in the boundary-layer region and Lagrangian outside.[4] Since boundary layers are simulated, the flow separates of its own accord and separation positions need not be specified. Unfortunately, these methods tend to break down near sharp edges since very small length scales need to be specified (unless, for example, the real plane is transformed from a circle).

However, sharp edges do fix separation, and advantage has been taken of this in inviscid calculations where point vortices are introduced near the edges at successive time steps and then convected in a potential-flow calculation. The body is usually represented through a transformation and the zero-normal velocity condition for vortices is effected by the use of images. The strengths and positions of nascent vortices are determined by criteria for the rate of shedding of vorticity and by the Kutta condition applied in the transformed plane. Often only one condition has been used and the vortex position has been estimated (see Ref. 5 for a general review). Such an approach is potentially computationally more efficient than "complete" solutions.

It is desirable to generalize the latter method by representing the surface through a boundary-integral or "panel" method. For unsteady airfoil flows, Basu and Hancock[6] (BH) have represented the surface by a source sheet and a uniform vortex sheet that satisfies Kelvin's theorem as vorticity is shed into the flow. Flow at the trailing edge was governed by the Kutta condition; Bernoulli's equation was applied iteratively to produce zero pressure difference across the edge while ensuring that the nascent vortex was "force free." BH produced good results for unsteady airfoil motion and gust loading.

In this paper, the method of BH for airfoils (with one shedding edge) is extended to sharp-edged cylinders (with two shedding edges). The method is developed by satisfying different edge conditions through a more general procedure. As with BH, two edge conditions are satisfied directly, but now a third follows automatically while the approximation to a fourth is monitored continuously. The approximation to a further boundary condition is also monitored. The surface is represented by a vortex sheet only which is discretized so that velocities in the wake may be calculated efficiently by the vortex-in-cell method with good flow definition.

The generalized method is tested with an equilateral triangle and rectangular shapes for which experimental measurements at high Reynolds numbers ($>10^4$) are available. The use of a vortex decay factor to "tune" the model is also investigated.

Received Nov. 28, 1983; revision received July 16, 1984.

*Lecturer, Department of Engineering, Simon Engineering Laboratories.

Theoretical Formulation

To nondimensionalize flow characteristics, the incident velocity is set to one and the cylinder cross-flow dimension to two. Time is nondimensionalized by a length and velocity of unity.

Surface Vorticity Distribution

The representation of a body in potential flow by a surface source, vortex, or doublet distribution is common practice in fluid dynamics and has been reviewed thoroughly by Hunt.[7] For this application a vortex distribution is used so that it may be readily incorporated, in discrete form, into the vortex-in-cell method.

It may be shown that a surface vorticity distribution or vortex sheet must make the velocity on the inside of the sheet zero and the contour a streamline.[3,7] As a consequence the normal velocity is also zero. The velocity on the outside of the sheet is equal to the vortex sheet strength. In two dimensions the complex potential at a point $z=x+iy$ due to a vortex sheet round a contour C is given by

$$F(z)=\int_C -i\frac{\gamma(z')}{2\pi}e^{-i\alpha(z')}\ell n(z-z')\,dz' \qquad (1)$$

where z' is the position on the sheet at which the strength is $\gamma(z')$, and $\alpha(z')$ is the angle of inclination of the sheet to the real axis. γ may be calculated numerically by dividing C into a number of linear segments N. Satisfying the zero-tangential velocity condition at the midpoint of each segment generates a set of N simultaneous linear equations.

The velocity at z due to a linear segment with end points z_1' and z_2' is given by

$$u-iv=i\frac{\gamma(z')}{2\pi}e^{-i\alpha(z')}\ell n\left(\frac{z-z_2'}{z-z_1'}\right) \qquad (2)$$

If the external velocity at the midpoint of each segment is U_E+iV_E, to make the tangential velocity on the "inside" of

each segment zero, we require, for $i=1,N$

$$\sum_{j=1}^{N} \gamma_j K_{ij} = -U_{Ei}\cos\alpha_i - V_{Ei}\sin\alpha_i \tag{3}$$

or, in matrix form, $\boldsymbol{K}\boldsymbol{\gamma}=\boldsymbol{c}$. The "influence" matrix $\boldsymbol{K}$ depends only on the geometry of the surface and is inverted and stored before time stepping starts. $\boldsymbol{\gamma}$ is thus given by the tangential velocities due to the external flow through $\boldsymbol{\gamma}=\boldsymbol{K}^{-1}\boldsymbol{c}$.

To ensure that the net circulation in the flow is exactly zero (Kelvin's theorem), one of Eqs. (3) (for a given i) is replaced by

$$\sum_{j=1}^{N} \gamma_j \Delta s_j = -\Gamma_E \tag{4}$$

where Δs_j is the segment length and Γ_E the circulation in the external flow.[3] This also ensures that the matrix $\boldsymbol{K}$ is nonsingular.[3]

Introduction of Shed Vorticity

At each time step, vorticity is introduced into the flow at the sharp-edge separation positions as uniform vortex sheets that will be converted into point or discrete vortices for the vortex-in-cell method. The external flow that determines the surface vorticity distribution comprises all the shed vorticity in addition to the incident or onset flow. At a new time step, tangential velocities on the surface segments are calculated, using the vortex-in-cell method for previously shed vorticity, and then they are stored. The influence of nascent vortex sheets is added and their characteristics are adjusted until required edge conditions are satisfied, as described below.

The Kutta condition has been discussed at length by BH. The essential requirement is that the singularity at the edge should be removed and this entails no force across the edge or on the sheet leaving the edge. Using the notation in Fig. 1 the Bernoulli equation across the edge is given by

$$\frac{p_s}{\rho}+\frac{1}{2}q_s^2+\frac{\partial\phi_s}{\partial t}=\frac{p_w}{\rho}+\frac{1}{2}q_w^2+\frac{\partial\phi_w}{\partial t} \tag{5}$$

where p is the pressure, q the total velocity, and ϕ the velocity potential.

We require $p_s=p_w$ and $q_s=0$, giving

$$\frac{\partial}{\partial t}(\phi_s-\phi_w)=\frac{1}{2}q_w^2 \tag{6}$$

Following BH,

$$\frac{\partial\Gamma}{\partial t}=\frac{1}{2}q_w^2 \tag{7}$$

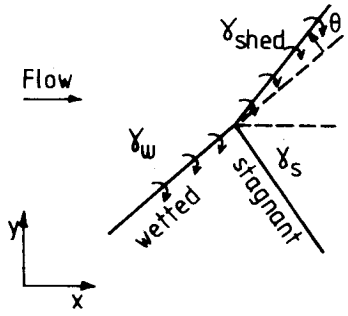

Fig. 1 Definition sketch of shedding edge.

Eq. (7) states the well-known result for the rate of shedding of vorticity from a wetted surface. We also require

$$\gamma_{\text{shed}}=\gamma_s+\gamma_w=\gamma_w \tag{8}$$

Within the limits of a numerical procedure with surface segments, q, p, and γ are evaluated at the midpoints of the edge segments (which will be made relatively small). BH did not enforce Eq. (8) or the $q_s=0$ condition, but proceeded using Eq. (5) in the form

$$q_w^2=q_s^2+2\frac{\partial\Gamma}{\partial t} \tag{9}$$

Zero pressure difference across the edge was maintained through an iterative procedure but no information was given on q_s, γ_{shed} and γ_w. BH used a source sheet with a uniform vorticity distribution superimposed to represent the surface and included the orientation of the shed segment as an unknown. After convergence the nascent sheet was always virtually tangential to the wetted surface (except when $q_s=q_w$).

For sharp-edged cylinders it is easy to imagine an initial situation with $q_s=q_w$ so that, based on Eq. (9), the method would break down. To avoid this (while ensuring rapid convergence in general) and to ensure a third edge condition, a scheme which enforces the conditions $q_s=0$ and $\gamma_w=\gamma_{\text{shed}}$ is adopted here. The condition of zero force across a shedding edge is automatically satisfied.

At a new time step, surface tangential velocities due to the onset flow and previously shed vortices are calculated and stored as mentioned above. For the first few time steps, a nascent sheet is introduced tangential to the wetted surface with a first estimate for strength of $0.7\gamma_w$ (as a result of numerical experiment) and length $0.7|\gamma_w|\Delta t/2$, since the convection velocity of a sheet is the mean of the velocities on either side. The influence of nascent sheets is now included in the surface tangential velocities using Eq. (2) and the new surface vorticity distribution is calculated.

The strength of a shed sheet is corrected to

$$\gamma_{\substack{\text{shed}\\\text{new}}}=\gamma_{\substack{\text{shed}\\\text{old}}}(1+0.5\gamma_s/\gamma_w) \tag{10}$$

to bring γ_s closer to zero. In addition, the condition $\gamma_w=\gamma_{\text{shed}}$ will not, in general, be satisfied. This is improved by adjusting the angle of the shed sheet. The angle θ in Fig. 1 is adjusted to

$$\theta_{\text{new}}=\theta_{\text{old}}+1.0(\gamma_{\text{shed}}-\gamma_w)/(|\gamma_w|+|\gamma_{\text{shed}}|) \tag{11}$$

to make $|\gamma_{\text{shed}}-\gamma_w|$ smaller. These equations are applied together and always correct γ_{shed} and θ in the "right" direction; factors 0.5 and 1.0 are a result of numerical experiment and certainly could be optimized further. Correspondingly, the segment length is corrected to $|\gamma_{\text{shed}}|\Delta t/2$. The process is repeated until $|\gamma_{\text{shed}}-\gamma_w|$ and $|\gamma_s|$ are less than 1% of the incident velocity, 50% for the first few time steps (usually four). After the first four time steps, values of γ_{shed} and θ from the previous time level are used as initial guesses. The iterative scheme is extremely efficient; the number of iterations has a negligible effect on computer time and approximately 10 iterations are often required.

Each nascent sheet (together with each sheet segment representing the surface) is divided into equispaced point vortices of equal strength to create at least two vortices per cell of inner mesh for the convection calculation described below. After a sheet has been in the flow in this form for a time greater than 10 it is reduced to a single vortex at its centroid of circulation. This combination always occurs well away from the surface and keeps the number in the flow down to a convenient level.

If a nascent sheet is to be force free (on average), its inclination to the x axis should be equal to that of the velocity vector

at its midpoint. This condition is not enforced, as it was by BH, and the difference in angles is output at each time level.

The Vortex-in-Cell Method

The vorticity equation in inviscid flow, $D\omega/Dt=0$, simply describes the convection of vorticity without diffusion. In a Lagrangian scheme discrete vortices are thus convected without changing their strength. The velocity of a vortex may be obtained by summing the influence of the other vortices and the onset flow. However, this is computationally prohibitive for a large number of vortices, say, 10^2 to 10^4. The vortex-in-cell method may handle such numbers efficiently and the method used here is identical to that described by Stansby and Dixon.[3] Overlapping rectangular meshes with square cells are set up for the solution of $\nabla^2\psi=-\omega$ in finite difference form using fast Fourier transforms, where ψ is the stream function and ω the vorticity. A mesh with a small cell size is desirable to cover the cylinder, an intermediate cell size is used for vortex sheet rollup, and a large cell size is adequate to transport large structures downstream. The coarsest mesh contains all of the vortices, the net circulation being zero. These vortices are some distance from the outer boundary where the stream function (due to vortices alone) is set to zero. The cell size is typically 0.4.[3] The boundary approximation may be tested from time to time by directly summing the influence of all of the vortices; however, this is extremely expensive in computer time. The stream function distribution on the outer mesh is obtained and gives the boundary values for the intermediate mesh by linear interpolation. Its vorticity distribution is produced by all of the vortices within the mesh which typically has a cell size of 0.1.[3] The stream function distribution for this mesh is then obtained and gives the boundary values for the inner mesh which is then solved in the same way. The velocity at a point is given by the ψ distribution from the mesh with the smallest cell size possible. A cell size of 0.025 for the inner mesh is adequate.

Vortices are moved by a second-order predictor-corrector scheme for which

$$x(t+\Delta t)=x(t)+\{U+0.5[u(t)+u']\}\Delta t \tag{12a}$$

$$y(t+\Delta t)=y(t)+\{V+0.5[v(t)+v']\}\Delta t \tag{12b}$$

where U and V are the onset velocities in the x and y directions (u and v are due to the vorticity alone), Δt the time step, and u' and v' the velocities at

$$x'=x(t)+[U+u(t)]\Delta t \tag{13a}$$

$$y'=y(t)+[V+v(t)]\Delta t \tag{13b}$$

The use of the vortex-in-cell method will not be discussed further herein but the reader may refer to Ref. 8 for rollup calculations and Ref. 9 for further rollup calculations and extensive investigations on the representation of surface vorticity distributions.

Pressure and Force

Pressures are calculated on the cylinder surface through the Euler equation

$$\frac{\partial u_s}{\partial t}+u_s\frac{\partial u_s}{\partial s}=-\frac{1}{\rho}\frac{\partial p}{\partial s} \tag{14}$$

where s is the distance around the surface and u_s the tangential velocity on the surface (in a counterclockwise sense). With the surface represented only by a vortex sheet, u_s is given directly by the vortex sheet strength γ_s and the vortex-in-the-cell method need not be applied. If $s=s_0$ when $p=p_0$

$$\frac{1}{\rho}(p-p_0)=-\int_{s_0}^{s}\frac{\partial u_s}{\partial t}ds-\frac{1}{2}(u_s^2-u_{s_0}^2) \tag{15}$$

If conditions are known at time t, pressures are calculated at time $(t-\Delta t)$ using the central difference formula for $\partial u_s/\partial t$.

γ_s is known at the segment midpoints and the integral in Eq. (15) is evaluated at the segment ends by the trapezoidal rule. A midsegment value is obtained simply by taking the average of the values at the segment ends. The pressure variation between two shedding edges is obtained through Eq. (15) with s_0 at the segment midpoint adjacent to the first shedding edge. There is a flow discontinuity across any shedding edge but the criteria for the introduction of vorticity causes the pressure difference to be zero (within numerical limitations). The pressures across the second shedding edge are thus equated and Eq. (15) is applied until the next shedding edge is reached. The pressure should return to its original value once a circuit has been completed and the "closing error" is output at each time step.

Results

A number of numerical parameters can be varied. The time step, cell size, and length of the shedding segment on the cylinder should not affect the results provided they are small enough. The surface sheet segments were given a length of about 0.1 and the two segments on either side of an edge were further divided into four (or eight) segments. In the final version each shedding segment was again divided into four segments; shedding segment lengths of 0.025, 0.0125, and 0.0062 were thus tested. Time steps of 0.2, 0.1, and 0.05 were tested and 0.1 was found to be small enough. Meshes of 129×129, 65×41, and 129×65 were used with cell sizes of 0.025, 0.1, and 0.4, respectively.

A rectangle with side dimensions of 0.4 will be referred to as the 0.2 rectangle (0.2 being the ratio of side to front dimensions); similarly, there will be a 0.6 rectangle. The sharp edges at the base of a rectangle were artificially smoothed to reduce unreallstically sharp changes in pressure. (Vorticity is shed only from the two upstream edges.) The flow was made asymmetric by introducing a normal incident velocity $0.5(1-t/2)$ for $0\leq t<2$. Maintaining recirculating vortices at 0.05 or 0.1 from the surface had little effect on the results and, subsequently, 0.1 was used.

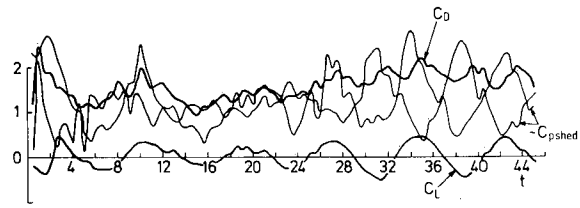

Fig. 2 Variation of drag and lift coefficient and pressure coefficient at the shedding edges of the triangle.

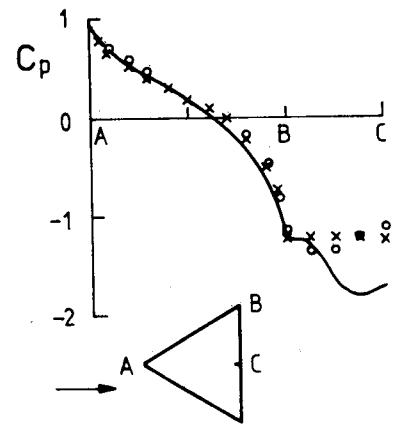

Fig. 3 Mean pressure coefficient distribution on the triangle: ——, no decay factor ($\beta=0$); o o o, $\beta=0.03$; and × × ×, experiment.[10]

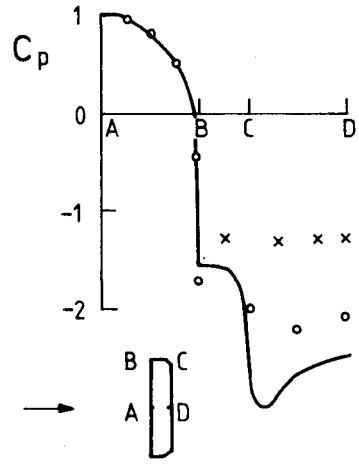

Fig. 4 Mean pressure coefficient distribution on the 0.2 rectangle: ——, no decay factor ($\beta=0$); o o o, $\beta=0.03$; and × × ×, experiment.[12]

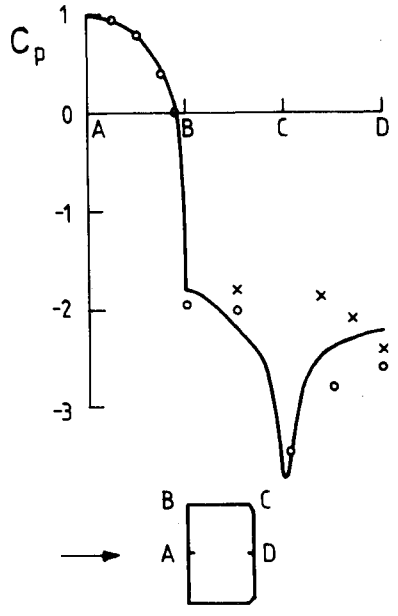

Fig. 5 Mean pressure coefficient distribution on the 0.6 rectangle: ——, no decay factor ($\beta=0$); o o o, $\beta=0.03$; and × × ×, experiment.[12]

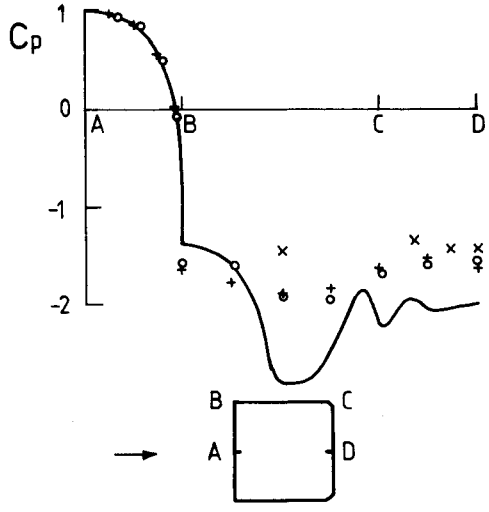

Fig. 6 Mean pressure coefficient distribution on the square: ——, no decay factor ($\beta=0$); o o o, $\beta=0.03$; × × ×, experiment.[12]; and + + +, experiment.[13]

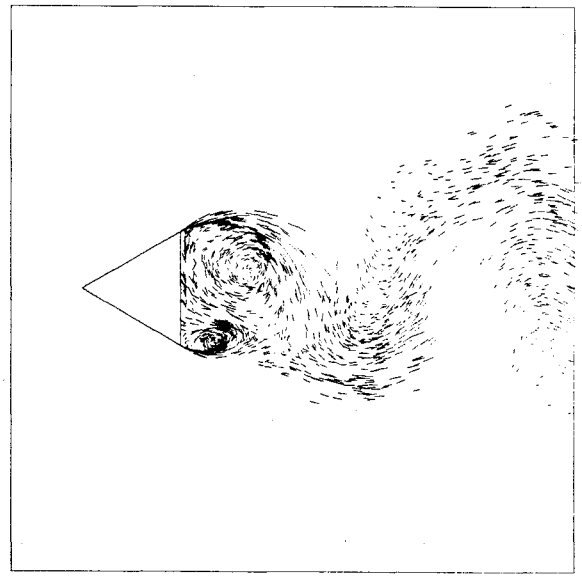

Fig. 7 Flow around the triangle at $t=45$. A dash shows vortex movement in one time step.

The representation of a surface by a vortex sheet causes zero velocity inside the surface in theory. The numerical approximation using the vortex-in-cell method has been shown to be accurate for the circular cylinder[3,9] and a check on the triangle showed that velocities inside the surface were less than 1% of the incident velocity.

Variations of the lift, drag, and pressure coefficient on the shedding segments show that wake behavior becomes periodic after about $t=25$ and, in general, mean drag is overestimated. The example of the triangle is shown in Fig. 2 where the mean drag coefficient of 1.8 compares with an experimental value of 1.4,[10] while the Strouhal number of 0.25 (obtained from the fluctuating lift) compares with 0.2.[10] The mean pressure coefficient distribution in Fig. 3 shows the reason the drag is overestimated; the central base pressure is clearly too low, while the pressures upstream of separation are predicted reasonably well. (The experimental results have been corrected for blockage.) The unrepresentative results are almost certainly because vorticity is rolling up too tightly in the wake causing unrealistically high velocities and, hence, low pressures at the base.

A real flow contains small- and large-scale three dimensionality. This has been assumed to cause an effective reduction in vortex strength in a two-dimensional simulation and has been modeled, without mathematical justification, by decaying vortex strength.[11] In this study, an exponential decay was tested by putting vortex strength $\Gamma=\Gamma_0 e^{-\beta t}$, where t is the age and Γ_0 the strength at creation, and varying β. β is in fact a balancing parameter; increasing β increases the rate of shedding of vorticity into the wake by reducing the vorticity in the wake. $\beta=0.03$ was found to be the optimum value (about half that used in Ref. 11) and gives the improved pressure distribution shown in Fig. 3.

Results for the 0.2 rectangle are far less satisfactory. The mean drag coefficient of 3.5 compares with an experimental value of 2.2[12] and a Strouhal number of 0.19 with 0.13.[12] The pressure coefficient distribution in Fig. 4 shows that the cause again lies in the base region and, in this case, the decay factor provides only limited improvement. There is an incomplete experimental pressure distribution for this shape and the 0.6 rectangle.

For the 0.6 rectangle the mean drag coefficient of 3.5 compares with 3.0[12] and the Strouhal number of 0.17 with 0.14.[12] The mean pressure coefficient distribution in Fig. 5 has features similar to the 0.2 rectangle with the decay factor again providing little improvement.

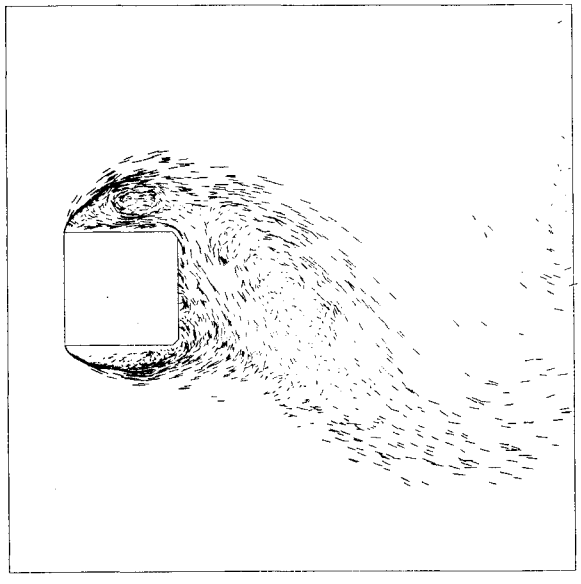

Fig. 8 Flow around the square at $t = 40$. A dash shows vortex movement in one time step.

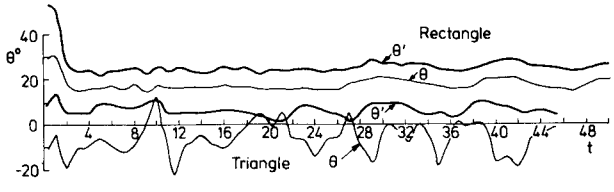

Fig. 9 Variation of angles of nascent sheet θ and its midpoint velocity vector θ' for lower edges of the 0.2 rectangle and triangle.

For the square the mean drag coefficient of 2.7 compares with 2.5[13] and the Strouhal number of 0.13 is in agreement with experiment.[13] Mean and fluctuating pressures have been measured around the surface[13] and Fig. 6 shows the mean pressures to be in fair agreement. Fluctuating pressures and forces were about 50% higher than experiment. In this case the decay factor brings the results into close agreement with experiment.

Flow pictures for the triangle and square are shown in Figs. 7 and 8. Tight rolling up can be seen for the triangle, while the afterbody controls vorticity interaction to some extent for the square.

Finally the approximation to two boundary conditions is described. The angle of inclination of the shed sheet θ and of the velocity vector at its midpoint θ' are plotted in Fig. 9 for the lower edges of the triangle and the 0.2 rectangle, θ is as shown in Fig. 1. The angles are not equal and tangential to the shedding edge as was found in the airfoil study of BH. The length of shedding segment was varied for the 0.2 rectangle and affected θ and θ' as shown in Table 1. However, the shedding pressure and other results were affected only slightly, although pressure always varied sharply just upstream of the shedding segment. A shedding segment length of about 0.0062 was used for all of the results shown here.

Thus, in general, the zero-force condition on a nascent sheet cannot be satisfied with the same precision as the other edge conditions. A linear nascent sheet represents a curved sheet in some mean way and perhaps it is unreasonable to expect very close agreement for the size of the time step used for practical reasons. In all other respects, the time steps appear to be adequately small.

The second approximate boundary condition is concerned with the pressure closure described above. After integration around the surface the "closing errors" in the pressure coefficient were always less than 0.2 and usually well below 0.1; these are thought to be acceptably small.

Table 1 Effect of length of shedding segment Δ_{shed} on angle of sheet θ and on angle of velocity vector at its midpoint θ' for lower edge of 0.2 rectangle

Δ_{shed}	0.00625	0.0125	0.025
θ, deg	18	24	34
θ', deg	25	24	28

Discussion and Conclusions

The main contribution of this paper is the improved scheme for introducing vortex sheets from sharp-edged cylinders represented by the panel method; vortex sheets in this case. The iterative scheme is efficient, robust, and general. A nascent sheet is not always tangential to the shedding segment as it was for Basu and Hancock.[6] This is probably because the shedding segments are at greater angles to the incident velocity, and possibly because new edge conditions are satisfied. (In the time-step limit $\Delta t = 0$ one would expect a nascent sheet to become tangential.)

The method is applied to cylinders rather than airfoils, partly to test the method with two shedding edges. Results are somewhat mixed, mainly because shear layers roll up too tightly in the model. Where complete pressure distributions are available, for the triangle and the square, pressures upstream of separation are predicted reasonably well, while base pressures are too low. In both cases a small vortex decay factor brings base pressures into close agreement with experiment, but the same factor gives little improvement for the 0.2 and 0.6 rectangles. The tight rolling up causes the Strouhal number to be high except for the case of the square, where the afterbody appears to control the shear-layer motion and subsequent interaction to some extent.

For the 0.2 and 0.6 rectangles the pressure distributions indicate very high velocities at the base edges and secondary shedding would clearly occur in reality. An attempt to apply the present technique for introducing vorticity to such edges broke down due to the extreme unsteadiness of the flow. Confronted with similar problems for the circular cylinder, Stansby and Dixon[14] found that approximating secondary shedding had two effects. Secondary vorticity was of opposite sign to the "primary" vorticity which creates it by rolling up close to cylinder. But it also caused the primary vorticity to roll up further from the base, thereby reducing velocities on the base and, hence, the strength of secondary shedding. To some extent, the decay factor will compensate for the lack of secondary shedding as well as three-dimensional effects. There is a dilemma in that a complete solution (e.g., Refs. 3 and 4) is desirable for the highly unsteady base region, while the present idealization is suited to sharp edges. The present method may be expected to give good results when secondary effects are known to be insignificant.

References

[1] Jordan, S. K. and Fromm, J. E., "Oscillatory Drag, Lift and Torque on a Circular Cylinder in a Uniform Flow," *The Physics of Fluids*, Vol. 15, March 1972, pp. 371-376.

[2] Chorin, A. J., "Numerical Study of Slightly Viscous Flow," *Journal of Fluid Mechanics*, Vol. 57, March 1973, pp. 785-796.

[3] Stansby, P. K. and Dixon, A. J., "Simulation of Flows Around Cylinders by a Lagrangian Vortex Scheme," *Applied Ocean Research*, Vol. 5, July 1983, pp. 167-178.

[4] Spalart, P. R., Leonard, A., and Baganoff, D., "Numerical Simulation of Separated Flows," NASA TM 84328, Feb. 1983.

[5] Leonard, A., "Vortex Methods for Flow Simulation," *Journal of Computational Physics*, Vol. 37, Oct. 1980, pp. 289-335.

[6] Basu, B. C. and Hancock, G. J., "The Unsteady Motion of a Two-Dimensional Aerofoil in Incompressible Inviscid Flow," *Journal of Fluid Mechanics*, Vol. 87, July 1978, pp. 159-178.

[7]Hunt, B., "The Mathematical Basis and Numerical Principles of the Boundary Integral Method for Incompressible and Potential Flow over 3-D Aerodynamic Configurations," *Numerical Methods in Applied Fluid Dynamics*, Academic Press, London, 1980, pp. 49-135.

[8]Baker, G. R., "The Cloud-in-Cell Technique Applied to the Roll-Up of Vortex Sheets," *Journal of Computational Physics*, Vol. 31, April 1979, pp. 76-95.

[9]Dixon, A. G. and Stansby, P. K., "The Cloud-in-Cell Method of Flow Simulation with Surface Vorticity Distributions," North West Universities Consortium for Marine Technology, Manchester, U.K., Rept. NW/M/1.3B/1, April 1983.

[10]Twigge-Molecey, C. F. M. and Baines, W., "Aerodynamic Forces on a Triangular Cylinder," *Journal of Engineering Mechanics*, Vol. 99, No. EM4, Aug. 1973, pp. 803-818.

[11]Sarpkaya, T. and Shoaff, R. L., "An Inviscid Model of Two-Dimensional Vortex Shedding for Transient and Asymptotically Steady Separated Flow Over a Cylinder," *AIAA Journal*, Vol. 17, Nov. 1979, pp. 1193-1200.

[12]Bearman, P. W. and Trueman, D. M., "An Investigation of the Flow Around Rectangular Cylinders," *Aeronautical Quarterly*, Vol. 23, Aug. 1972, pp. 229-237.

[13]Bearman, P. W. and Obasaju, E. D., "An Experimental Study of Pressure Fluctuations on Fixed and Oscillating Square-Section Cylinders," *Journal of Fluid Mechanics*, Vol. 119, June 1982, pp. 297-321.

[14]Stansby, P. K. and Dixon, A. G., "The Importance of Secondary Shedding in Two-Dimensional Wake Formation at Very High Reynolds Numbers," *Aeronautical Quarterly*, Vol. 33, May 1982, pp. 105-122.